Microchimica Acta (2020) 187: 554
https://doi.org/10.1007/s00604-020-04537-8

ORIGINAL PAPER

Paper chip-based colorimetric assay for detection of *Salmonella typhimurium* by combining aptamer-modified Fe_3O_4@Ag nanoprobes and urease activity inhibition

Shengnan Wei[1] · Juan Li[1] · Jingya He[2] · Wei Zhao[3] · Feng Wang[2] · Xiuling Song[1,4] · Kun Xu[1,4] · Juan Wang[1] · Chao Zhao[1]

Received: 26 March 2020 / Accepted: 28 August 2020 / Published online: 9 September 2020

Abstract

A rapid and sensitive colorimetric assay is described for *Salmonella typhimurium* (*S. typhimurium*) detection using urea/phenol red impregnated test paper. Aptamer-modified Fe_3O_4@Ag multifunctional hybrid nanoprobes (apt-Fe_3O_4@Ag NPs) were used to specifically captured *S. typhimurium*; the nanoprobes were quickly etched by H_2O_2 to form Ag^+. The generated Ag^+ can inhibit the urease-catalyzed hydrolysis reaction of urea to produce NH_4^+. Consequently, the as-prepared test paper displayed a yellow color. In the presence of *S. typhimurium*, the target bacteria can cause aggregation of apt-Fe_3O_4@Ag NPs, and the deposited Ag on the nanoprobe's surface is shielded against H_2O_2-induced oxidative decomposition leading to reduced Ag^+ production. The catalytic activity of urease cannot be inhibited completely by inadequate amount of Ag^+. An obvious color change from yellow to pink can be monitored directly using our test paper as a result of increased NH_4^+. The entire assay procedure could be completed within 1 h. A limit of detection of 48 cfu/mL is achieved with a linear range of 1×10^2 to 1×10^6 cfu/mL. The recoveries of *S. typhimurium* spiked in pure milk samples were 92.48–94.05%.

Keywords Food safety · Foodborne pathogen · Visual detection · Immunomagnetic separation · Urea/phenol red impregnated paper · Ag^+-mediated urease activity inhibition

Introduction

Foodborne diseases have been considered among the most important public health problems worldwide [1], and the number of foodborne disease incidences rises significantly in recent years [2]. *Salmonella* is widely known as one of the most prevalent pathogens causing foodborne illness outbreaks [3]. *Salmonella* contaminates food products, like eggs, fruits, vegetables, meat, poultry, and milk, typically through animal fecal contamination [4]. According to the World Health Organization, diarrheal diseases are the most common illnesses resulting from unsafe food, 550 million people falling ill each year, including 220 million children under the age of 5 years. Salmonella is 1 of the 4 key global causes of diarrheal diseases [5]. So there is an urgent need to detect *Salmonella* at pre-infectious levels. At present, traditional culture-based methods for the detection of *S. typhimurium* are laborious and time-consuming, often taking 3–5 days to obtain a result [6]. The need for expensive equipment and trained lab personnel increases detecting costs, making large-scale studies of *Salmonella* epidemiology hard [7]. To achieve the rapid and sensitive requirements for *S. typhimurium* detection, numerous culture-independent techniques have been developed including polymerase chain reaction (PCR) [8], fluorescence [9], electrochemistry [10], surface plasmon resonance (SPR)

Electronic supplementary material The online version of this article (https://doi.org/10.1007/s00604-020-04537-8) contains supplementary material, which is available to authorized users.

✉ Juan Li
li_juan@jlu.edu.cn

✉ Juan Wang
jwang0723@jlu.edu.cn

✉ Chao Zhao
czhao0529@jlu.edu.cn

[1] School of Public Health, Jilin University, Changchun 130021, China

[2] School of Stomatology, Jilin University, Changchun 130021, China

[3] Jilin Provincial Center for Disease Control and Prevention, Changchun 130062, China

[4] Public Health Detection Engineering Research Center of Jilin Province, Changchun 130021, China

[11], and so on. Although all the methods mentioned above are accuracy and sensitive, they need expensive and sophisticated equipment and complicated sample preparation while having time-consuming steps. Accordingly, it is crucial to develop simple, inexpensive, and effective methods to detect *S. typhimurium* in contaminated food samples.

Over the past decade, paper-based analytical devices (PADs) have been successfully developed. The properties of PADs are small sample, reagent consumption, disposability, and portability [12]. PADs hold great potential for using as analytical tools in remote areas. These advantages make PADs attractive for detection in fields such as environmental monitoring, medical diagnostics, point-of-care testing, and food safety control [13]. However, there have been only a few reports on using PADs for rapid detection of bacteria. Although different PAD methods possess their own features and gives the different insights, these methods usually suffer from some inevitable defects such as complicated test paper preparation and time-consuming. For example, paper-based ELISA are often employed for point-of-care diagnostic analysis of bacteria, but most of paper-based ELISA still tolerate their expensive antibody, complicated paper preprocessing and background interference [14, 15]. PADs based on species-specific enzyme of bacteria are of limited use for on-site applications as they are time-consuming on pretreatment sample process and rely on bacterial activity [16]. PAD based on bacterial glucose metabolism is nonspecific, and the color change of this PAD is indistinguishable because of the method used starch-iodide paper as substrate [17]. Therefore, the development of simple and legible test paper for bacteria detection is strongly desired.

Magnetic composite microspheres have been extensively explored because of their applications in the biomedical field [18]. In particular, magnetic composite microspheres possess strong magnetic responsiveness owing to their micro-scale magnetic core, which is more suitable than magnetic nanoparticles for bio-separation [19]. Magnetic nanoparticles are not easily modified by aptamer or antibody because they have few modifiable sites and magnetic attraction often brings in aggregation among particles to lose magnetic properties [20]. In order to overcome this limitation, the magnetic Fe_3O_4@Ag nanocomposites have been developed. Due to the multifunction of the nanocomposites, Fe_3O_4@Ag not only possesses magnetic separation ability but also is prone to modification. The Fe_3O_4@Ag with fast response and high sensitivity has been served as the target capture tool and the SERS or electrochemical signal amplification platform [21, 22]. But up to now, to our knowledge, the Fe_3O_4@Ag nanocomposites have not been applied in bacteria colorimetric detection.

In this study, we developed a rapid and sensitive colorimetric assay for *S. typhimurium* detection using multifunctional hybrid nanoprobes and urea/phenol red impregnated paper. To selectively recognize the target, the multifunctional hybrid nanoprobes were synthesized and modified with specific aptamer via Ag-S bond (apt-Fe_3O_4@Ag NPs). Through etching of silver shell coated on the apt-Fe_3O_4@Ag NPs to regulate the catalytic activity of urease [23, 24], the multifunctional hybrid nanoprobes conversed the signal of the number of *S. typhimurium* to the color change of as-prepared test paper as a result of pH value change. Therefore, an obvious color change from yellow to pink can be monitored directly. The entire assay procedure can be completed within 1 h without pre-enrichment and any sophisticated instrument. Herein, apt-Fe_3O_4@Ag NPs are not only intended for enrich and magnetic separation of *S. typhimurium*, but also its silver shell can be used as the reaction substrate to realize the output of detection signals. Compared with "sandwich assays" with two or more nanoprobes [25, 26], multifunctional apt-Fe_3O_4@Ag NPs made the operation simpler and faster. Furthermore, the combination of smartphone technology and colorimetric paper-based sensing platform can enable simple inexpensive diagnostics.

Experimental details

Materials and reagents

Ferric chloride hexahydrate ($FeCl_3 \cdot 6H_2O$), trisodium citrate, sodium acetate (NaAc), acetone, and hydrogen peroxide (H_2O_2) were from Beijing Chemical Reagent Co., Ltd. (China). Urease and Poly-vinylpyrrolidone ($PVP_{k\text{-}30}$) were from Shanghai Yuanye Bio-Technology Co., Ltd. (China). Ethylene glycol was from Tianjin Fuyu (China). Silver nitrate ($AgNO_3$) and tris (2-carboxyethyl) phosphine hydrochloride (TCEP) were received from Aladdin (China). Urea was purchased from Sigma-Aldrich (USA). Phenol red was from Macklin (China). Thiolated anti-*S. typhimurium* aptamers were obtained from Sangon Biotech (Shanghai) Co., Ltd. (China) with the following sequences [27]: 5′-SH-$(CH_2)_6$-TAT GGC GGC GTC ACC CGA CGG GGA CTT GAC CTT GAC ATT ATG ACA G-3′.

The pH-neutral (pH = 7.2) double distilled water (DDW) and phosphate-buffered saline (PBS, 0.01 mol L^{-1}, pH = 7.4) were prepared by us. The test paper with phenol red and urea was homemade. Briefly, the neutral cotton filter paper (Aoke, China) was completely soaked by a 60% (w/v) ethanol solution containing 0.1% (w/v) phenol red and 0.5 M urea. After drying, the treated paper should be stored in the sealed, cool, dark, and dry condition.

Synthesis of Fe_3O_4@Ag nanoparticles

Firstly, the Fe_3O_4 magnetic particles were synthesized through a modified solvothermal reaction as previously reported [28]. $FeCl_3 \cdot 6H_2O$ (2.16 g, 8 mmol), trisodium citrate (0.5 g, 1.7 mmol), and sodium acetate ($NaAc \cdot 3H_2O$) (3.34 g, 24.4 mmol) were dissolved in ethylene glycol (40 mL) with magnetic stirring. The yellow solution was then transferred into a 100-mL Teflon-lined stainless-steel autoclave, heated at 200 °C for 10 h, and then cooled to room temperature. The black products were washed three times in ethanol and DDW, respectively. Finally, black Fe_3O_4 nanoparticles were stored in sealed and dry conditions for further use.

Fe_3O_4@Ag nanoparticles were synthesized by a solution-phase reduction that was adopted to protect growth under PVP on the surface of magnetic microspheres [29]. The prepared Fe_3O_4 particles (0.2 g) were dispersed in 24 mL of ethylene glycol containing silver nitrate (0.1 g) and $PVP_{k\text{-}30}$ (2.5 g) and then stirred for 12 h at 100 °C. Next, the silver nanoparticle embedded Fe_3O_4 particles (Fe_3O_4@Ag) were washed with acetone and DDW several times to remove ethylene glycol and $PVP_{k\text{-}30}$. Finally, the product was resuspended with DDW and stored at 4 °C for further uses.

Preparation of the apt-Fe_3O_4@Ag nanoprobes

The aptamers against *S. typhimurium* were modified onto the surface of Fe_3O_4@Ag based on a procedure reported in literature [30]. First, 10 μL of 10 μM aptamer was incubated with 1 μL of 1-mM TCEP buffer in the dark for 1 h for the reduction of disulfide bond of aptamer. Then, 1 mL of 1 $mg \cdot mL^{-1}$ Fe_3O_4@Ag solution was added to the deprotected aptamer and kept for 12 h for the assembling of Fe_3O_4@Ag to thiol group of aptamer segment. After that, apt-Fe_3O_4@Ag NPs were washed three times with DDW and resuspended in 500 μL of DDW. Finally, the products were stored at 4 °C without light for further uses.

Culture of bacteria

All the bacterial strains used in this study were provided by the Department of Hygienic Inspection, School of Public Health, Jilin University (Changchun, China). Five foodborne pathogenic bacterial strains stored at − 80 °C were used, including the target bacterium, *S. typhimurium* (ATCC 14028), and the four non-target bacteria, *Staphylococcus aureus* (ATCC 23213), *Listeria monocytogenes* (ATCC 43251), *Escherichia coli O157:H7* (ATCC 43888), and *Vibrio parahaemolyticus* (ATCC 17802).

All of them were revived on Luria-Bertani agar (LA) plates, except *Vibrio parahaemolyticus*, which was revived on LA plates with 3% (w/v) NaCl. After 24 h of inoculation, a single colony of each strain was picked up and grown in the corresponding medium at 37 °C with shaking at 180 rpm for 10 h. Subsequently, the bacteria were washed three times using sterile PBS by centrifugation at 5000 rpm for 10 min. After pour plate counting, it was diluted by sterile PBS aqueous solution.

Colorimetric detection of *S. typhimurium*

Bacteria samples with varying concentrations (from 1×10^2 to 1×10^6 cfu/mL) were prepared by diluting the freshly cultured bacteria with sterile PBS. The H_2O_2 solution was also diluted by sterile PBS. After optimization of experimental conditions, 900 μL of 10-fold serial dilutions of *S. typhimurium* were respectively added into sterile Eppendorf tubes containing 100 μL of 2 $mg \cdot mL^{-1}$ apt-Fe_3O_4@Ag NPs. For the negative control, 900 μL of sterile PBS without bacteria was used. The mixtures were incubated at room temperature shaken for 45 min. After magnetic separating for 2 min, 100 μL of 100 mM H_2O_2 was added to each tube to etch apt-Fe_3O_4@Ag-*S. typhimurium* complexes followed by magnetic separation for 2 min. Next, 5 μL of supernatant in each tube was taken to another one tube containing 10 μL of 50 U/mL urease. After 10 min of incubated at room temperature, the test paper was dipped with 2-μL reaction solution. The color change of test paper was recorded at the designated illuminated position by taking a photograph with a smartphone (Apple, USA).

Detection of *S. typhimurium* in real samples

Pure milk from the local supermarket was diluted 100-fold with sterile PBS and was artificially spiked with freshly cultured *S. typhimurium* at different levels (from 1×10^2 to 1×10^6 cfu/mL). The detection protocol was described in the section rapid colorimetric detection of *S. typhimurium* procedure for *S. typhimurium* detection, except that pure PBS buffer was replaced with milk samples.

Images and data analysis

The digital images of JPEG format files were imported into ImageJ (NIH, USA) software for further analyzing [31]. The largest "fittable" square was interactively drawn around each paper square in the dipstick image, and the RGB value of each reaction area was captured. Based on the RGB analysis, the gray value was calculated using a weighted average of red, green, and blue components using the eye sensitivity function ($gray\ value = 0.30 * R + 0.59 * G + 0.11 * B$) [32]. All the data were expressed as the means ± standard deviations ($x \pm SD$). Student's *t*-tests and analysis of variance (ANOVA) were conducted for the statistical analysis using SPSS Statistics software (version 22.0, IBM, USA). The analyses used a two-sided 0.05 significance level.

Results and discussion

The principle of colorimetric detection of *S. typhimurium*

In this study, a rapid and sensitive colorimetric assay for *S. typhimurium* detection using apt-Fe_3O_4@Ag NPs and urea/phenol red impregnated paper was developed. Scheme 1 illustrates the whole procedure. The high specific sequences of thiol-modified ssDNA aptamer against *S. typhimurium* were obtained from Joshi's work [27] and further immobilized to the surface of Fe_3O_4@Ag to form multifunctional hybrid nanoprobes (apt-Fe_3O_4@Ag NPs) by Ag-S bond. The apt-Fe_3O_4@Ag NPs is not only intended for enriching and magnetic separation of *S. typhimurium*, but also its silver shell can be used as the reaction substrate to realize the output of detection signals. The apt-Fe_3O_4@Ag NPs were specifically captured *S. typhimurium* as well as quickly were etched by H_2O_2 to produce Ag^+ through autocatalytic oxidation reaction of Ag nanoparticles [23]. The generated Ag^+ can inhibit the urease-catalyzed hydrolysis reaction of urea to produce NH_4^+, because the binding of the silver ions at the edge of the active site channel supposedly blocks the movement of the flap [24]. The urea/phenol red test paper is used as a carrier of colorimetric signal presentation. Consequently, the test paper displayed the original yellow color. In the presence of *S. typhimurium*, the apt-Fe_3O_4@Ag NPs can recognize and bound to the target bacteria to form apt-Fe_3O_4@Ag NPs-*S. typhimurium* complexes, leading to a large-scale aggregation toward to the target bacteria. Based on this phenomenon, the deposited Ag on the nanoprobes surface is shielded against H_2O_2-induced oxidative decomposition resulting in few Ag^+ production. Herein, the H_2O_2 is used to etch silver shell coated on the apt-Fe_3O_4@Ag NPs to regulate the catalytic activity of urease. The catalytic activity of urease is partially inhibited by inadequate amount of Ag^+. Different levels of etching of silver shell are corresponding to the different *S. typhimurium* concentration. Therefore, an obvious color change from yellow to pink could be monitored directly using our test paper as a result of NH_4^+ increased by urease-mediated the hydrolytic decomposition of urea. For quantitatively, the gray value was proportional to the *S. typhimurium* logarithm concentration.

Characterization of the apt-Fe_3O_4@Ag NPs

This core-shell structured apt-Fe_3O_4@Ag NPs has an Fe_3O_4 magnetic core and a layer of Ag nanoparticles' shell. Size analysis of particles in TEM images was carried out using the ImageJ software. We chose three inner diameters of every nanoparticle (total 50 nanoparticles) and take the average value. All the data were expressed as the means ± standard deviations (x ± SD). Figure 1a and b displayed the TEM photograph of Fe_3O_4 and Fe_3O_4@Ag microspheres with a mean

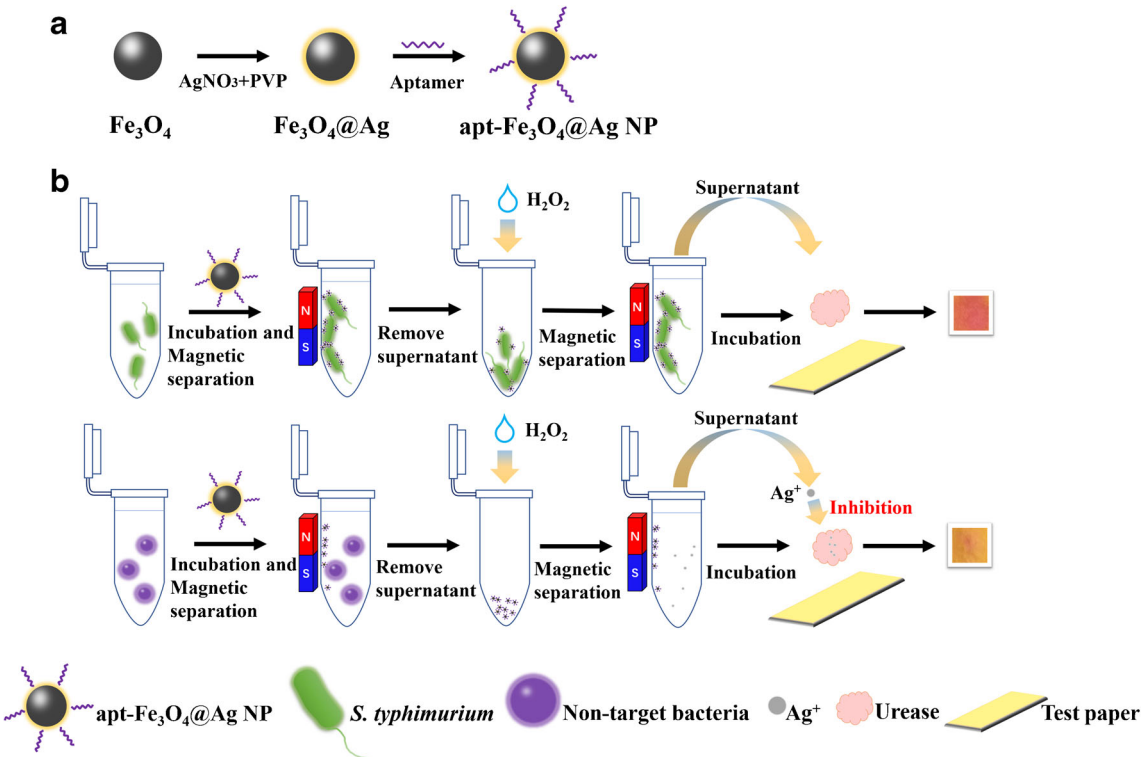

Scheme 1 Schematic diagram of the proposed colorimetric assay for *S. typhimurium* detection based on etching of bifunctional apt-Fe_3O_4@Ag NPs and inhibiting catalytic activity of urease by Ag^+

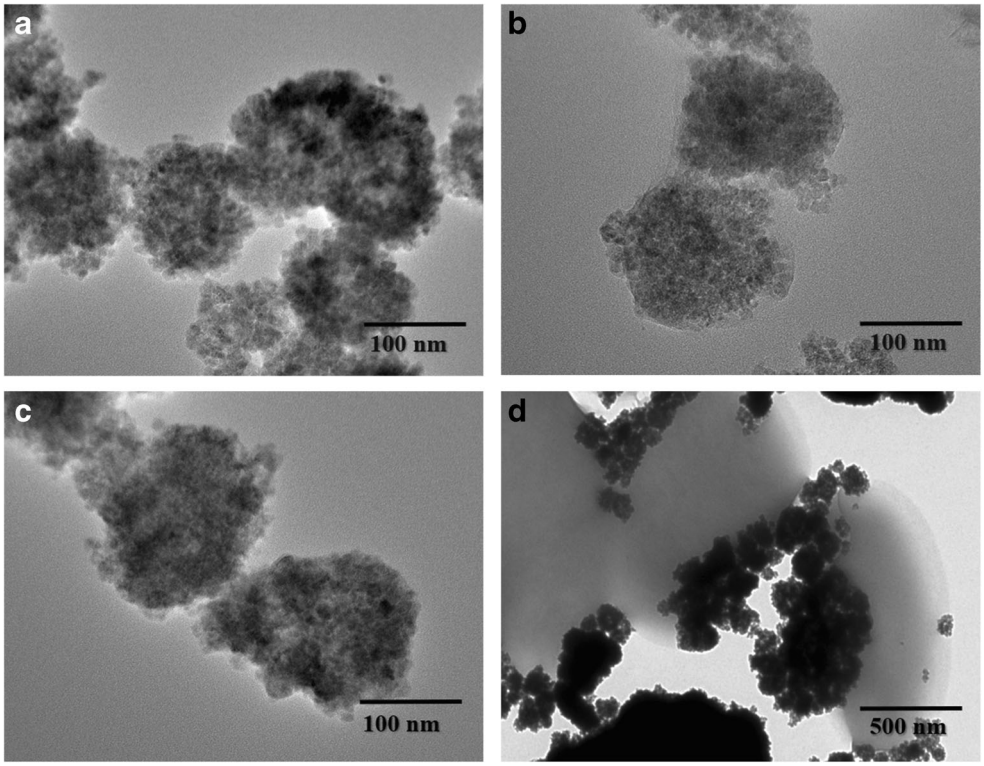

Fig. 1 TEM images of **a** Fe_3O_4, **b** Fe_3O_4@Ag, **c** apt-Fe_3O_4@Ag NPs, and **d** apt-Fe_3O_4@Ag NPs combined with *S. typhimurium*. In all samples, the final concentration of Fe_3O_4, Fe_3O_4@Ag, and apt-Fe_3O_4@Ag NPs is 0.2 mg·mL^{-1}. The final concentration of *S. typhimurium* is 1×10^6 cfu/mL

diameter of about 110 ± 4 nm and 130 ± 5 nm, respectively. As revealed in Fig. 1c, the apt-Fe_3O_4@Ag NPs microspheres were uniform with a size of approximately 131 ± 5 nm and 10 nm of Ag nanoparticle layer. Finally, the aggregations of apt-Fe_3O_4@Ag NPs were observed in Fig. 1d, which was due to the specific binding between lots of apt-Fe_3O_4@Ag NPs and *S. typhimurium* resulting in forming the apt-Fe_3O_4@Ag-*S. typhimurium* complexes [33].

To verify the formation of Ag nanocrystals in the microspheres, the X-ray diffraction (XRD) patterns of apt-Fe_3O_4@Ag NPs were recorded from $2\theta = 20°$ to 80°. As depicted in Fig. 2a, the position and relative intensities of peaks observed at 2θ of 30.5°, 35.9°, 43.4°, 57.6°, and 63.2° match perfectly to Fe_3O_4 with an inverse cubic spinal structure according to JCPDS data (card no. 75−1609). Diffraction peaks at 2θ of 38.3°, 44.5°, 65.1°, and 77.5°, which correspond to the (111), (200), (220), and (311) lattice planes of the face-centered cubic (*fcc*) phase of Ag (JCPDS no.04-0783), respectively [34].

In the UV-Vis spectrum (Fig. 2b), the Fe_3O_4@Ag microspheres exhibited an absorption peak at 402 nm that corresponds to a typical surface plasmon resonance band of silver nanoparticles. After modifying aptamer on the Fe_3O_4@Ag microspheres, the absorption peak shifted to 416 nm. The FTIR spectrum of apt-Fe_3O_4@Ag NPs was demonstrated in Fig. 2c. The obvious characteristic band at 586, 1454, 1612, and 3331 cm^{-1} could be attributed to the stretching vibration of Fe-O bond, C-N bond, C=O bond of peptide linkages, O-H and N-H bond could be attributed to the stretching vibration of Fe-O bond, C-N bond, C=O bond of peptide linkages, O-H and N-H bond, respectively [35]. The magnetic property of apt-Fe_3O_4@Ag NPs was examined using VSM magnetometry. As shown in Fig. 2d, the magnetic saturation (MS) value of Fe_3O_4, Fe_3O_4@Ag, and apt-Fe_3O_4@Ag NPs was 65.7 emu/g, 60.7 emu/g, and 57.1 emu/g, respectively. The decrease of MS indicates that silver shell deposited on Fe_3O_4 nanoparticles as expected. Moreover, the apt-Fe_3O_4@Ag NPs could be completely separated from the solution by an external magnet within 20 s, indicating that these apt-Fe_3O_4@Ag NPs had strong magnetic responsivity and were very suitable for efficient separation and enrichment of target molecules in solution.

Optimization of experimental conditions

In order to achieve the best experimental performance, subsequent experimental conditions were optimized, such as the concentration of etching agent, etching time, and incubation time for urease reacted with Ag^+. Respective data and figures were given in the ESM (Fig. S1–S3). The following experimental conditions were chosen to give the best results: (a) concentration of H_2O_2, 100 mM; (b) etching time, 10 min; and (c) incubation time, 2 min. In addition, the lifetime of apt-Fe_3O_4@Ag NPs and the test paper were investigated (Fig. S4). The results indicated that the apt-Fe_3O_4@Ag NPs could be used within 1 month after preparation in 4 °C condition, and the test paper was

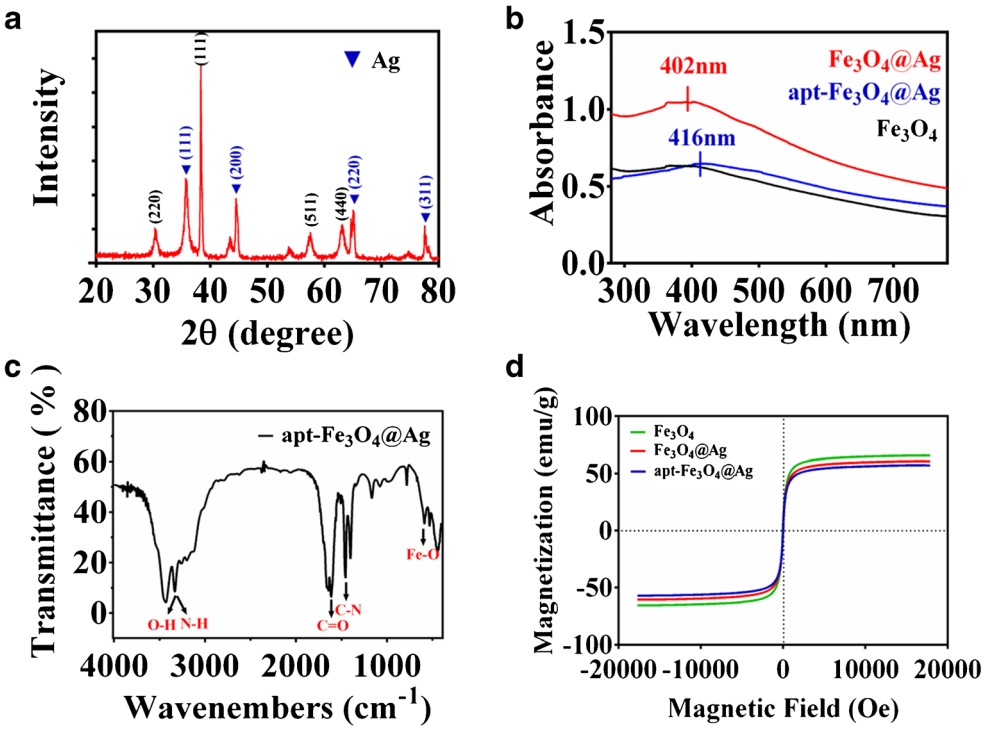

Fig. 2 **a** Wide-angle XRD pattern of apt-Fe_3O_4@Ag NPs, **b** UV-Vis spectra of Fe_3O_4, Fe_3O_4@Ag and apt-Fe_3O_4@Ag NPs, **c** the FTIR spectra of the apt-Fe_3O_4@Ag NPs, and **d** magnetic hysteresis curves of the Fe_3O_4, Fe_3O_4@Ag and apt-Fe_3O_4@Ag NPs. In all samples, the final concentration of Fe_3O_4, Fe_3O_4@Ag and apt-Fe_3O_4@Ag NPs is 0.2 mg/mL

recommended to be used within 9 months in a sealed, cool, dark, and dry condition.

Sensitivity and selectivity of the assay

Under the optimized conditions, varying concentrations of *S. typhimurium* (from 1×10^2 to 1×10^6 cfu/mL) were prepared by diluting the freshly cultured bacteria with sterile PBS. PBS was employed instead of *S. typhimurium* as a negative control (NC). Herein, only 80% of the area of the testing spot was considered in the measurement to prevent edge effects [36]. As presented in Fig. 3, with increasing of the concentration of *S. typhimurium*, the color of the test paper gradually changed from yellow to pink, revealing that the degree of etching of silver shell was reversely dependent on *S. typhimurium* level (the original image is in Fig. S5). The limit of detection (LOD) for *S. typhimurium* was determined to be 48 cfu/mL (3σ/slope, where σ is the standard deviation of 10 blank samples) [37]. Also, the RGB value of test papers was measured. Its gray value change could be well fitted by a linear function, $y = -7.249x + 151.5$, with a correlation coefficient of $R^2 = 0.985$, where x was the log scale of *S. typhimurium* count in cfu/mL (Fig. 3).

To investigate the selectivity of our proposed colorimetric method, the concentration of *S. typhimurium* was tested at 1×10^6 cfu/mL, and 4 other common bacterial strains at the concentration of 1×10^7 cfu/mL were detected as possible interfering species, including *E. coli O157:H7*, *L. monocytogenes*, *S. aureus*, and *V. parahaemolyticus*, and the sterile PBS sample was used as the reagent blank. First, each interfering bacterial strain was analyzed separately. Then the mixture of four interfering bacterial strain and the mixture of four interfering bacterial strain added *S. typhimurium* were analyzed. As shown in Fig. 4, a vivid color change from yellow to pink was observed in the presence of *S. typhimurium* alone and *S. typhimurium* mixed with other bacteria. As confirmed by the gray value, there was no statistically significant difference

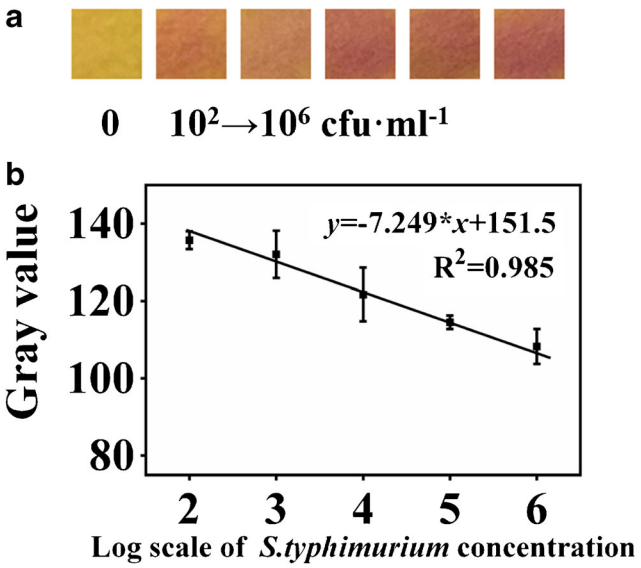

Fig. 3 **a** Photographs and **b** the proposed colorimetric assay after incubation with *S. typhimurium* at various concentrations (from 1×10^2 to 1×10^6 cfu/mL), the calibration curve for *S. typhimurium* (the gray value vs. the log scale of *S. typhimurium* concentration). All measurements were acquired at room temperature in PBS (pH 7.4). Error bars represent the standard deviation of three replicates

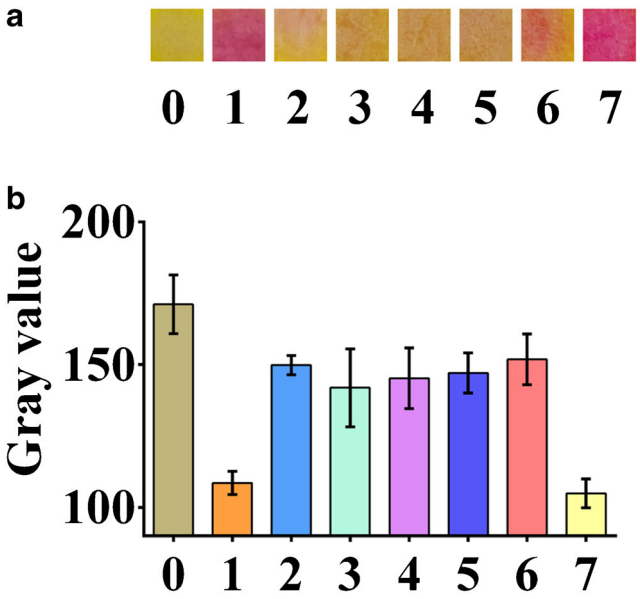

Fig. 4 Selectivity test. **a** Photographs and **b** the gray value of colorimetric results in the presence of different analytes (*S. typhimurium*, 1×10^6 cfu/mL; other bacteria, 1×10^7 cfu/mL) at pH 7.4 (0 → 7: blank, *S. typhimurium*, *S. aureus*, *L. monocytogenes*, *E. coli O157:H7*, *V. parahaemolyticus*, mixture, and mixture + *S. typhimurium*). Error bars represent the standard deviation of three replicates

between the negative samples and reagent control under the same conditions ($F = 0.822$, $p > 0.05$).

All the above results proved that our proposed method could achieve sensitive and selective *S. typhimurium* detection against potential interference.

Detection of *S. typhimurium* in real samples

The accuracy and applicability of our proposed method were further explored by conducting three replicate analyses of *S. typhimurium* in milk. The sterility of milk samples was verified by three replications by the plate culture method (Fig. S6). In order to reduce or eliminate matrix interferences completely, milk samples were diluted 100-fold with DDW and artificially spiked with various amounts of *S. typhimurium* (from 1×10^2 to 1×10^6 cfu/mL) to obtain the calibration curve. As expected, the linear range and the LOD for *S. typhimurium* were not interfered by matrix components (Fig. S7), which suggested that this method could be applied in milk samples analysis. The recoveries and relative standard derivations (RSDs) were further investigated and summarized in Table 1. Because samples of commercially available milk were uncontaminated, a known amount of *S. typhimurium* was spiked in each sample. All the average recoveries for different concentrations (1×10^2, 1×10^4, 1×10^6 cfu/mL) of *S. typhimurium* in milk samples were in the range of 92.48–94.05% with the RSDs lower than 10%. Simultaneously, it should be noted that a bare-eye distinguishable color was observed in all positive samples (Table 1). The LOD for *S. typhimurium* was determined to be 60 cfu/mL (3σ/slope, where σ is the standard deviation of 10 blank samples) in the milk. These results indicated that the setup method has a strong anti-interference ability for accurately evaluating *S. typhimurium* levels in complex food matrices.

As illustrated in Table S1, our proposed sensing methodology may be one of the most sensitive colorimetric assays comparable with the previous methods. Yi J et al. presented the CMCS-Apt-AuNP composites as molecular recognition elements to identify of *S. typhimurium* [37], where the carboxymethyl chitosan (CMCS) was only used as a carrier for target. However, apt-Fe_3O_4@Ag NPs has dual function involving magnetic separation of target and reaction as substrate in our study. Srisa-Art et al. reported a colorimetric PAD combined with an immunomagnetic separation (IMS) for detecting *S. typhimurium* [38]. This method is portable and sensitive but more time-consuming (90 min) than our assay method (< 1 h). Our entire analysis procedure could be completed within 1 h, including the incubation of apt-Fe_3O_4@Ag NPs with sample and magnetic separation (47 min), the etching apt-Fe_3O_4@Ag NPs' shell by H_2O_2 and magnetic separation (2 min), collecting free Ag^+ in the supernatant and the incubation of urease with Ag^+ (10 min), and coloration using urea/phenol red impregnated paper (about 10 s). However, there are some limitations of this approach. We also conducted a 100-fold interference experiment to explore the specificity with high concentration bacteria. As shown in Fig. S8, there was no significant difference between different bacteria with high concentration. It is due to the non-specific adsorption between excessive concentration of bacteria and nanoprobes that lead to poor specificity. To address this limitation, milk samples must be diluted many times before the method can be applied in practice. Obviously, the specificity of our method was almost not

Table 1 Recovery and RSD values of detecting *S. typhimurium* in milk samples ($\overline{x}, n = 3$)

Sample	Found (cfu/mL)	Added (log C, cfu/mL)	Found (log C, cfu/mL)	Recovery (%)	RSD (%)	Photography
Milk 1	BDL[a]	2	1.85	92.48%	5.46%	
Milk 2	BDL	4	3.84	95.99%	0.58%	
Milk 3	BDL	6	5.64	94.05%	5.05%	

[a] *BDL* below detection limit

interfered with the proper concentration of other bacteria (Fig. 4). The other restriction is the lack of high resolution of detection system when the color of the test paper had small changes, which is expected to find alternative material of the test paper to make the color change more distinguishable or employ more advanced equipment to obtain images. Overall, this proposed method could be expanded to the application in the other pathogens' detection by modifying the aptamer against different bacteria on Fe_3O_4@Ag NPs.

Conclusion

Herein, we have successfully developed a simple, rapid, and reliable colorimetric assay for *S. typhimurium* detection. Three main highlights were exhibited in this study: (1) The apt-Fe_3O_4@Ag NPs as multifunctional hybrid nanoprobes are not only intended for enrich and magnetic separation of target, but also its silver shell can be used as the reaction substrate in assay process; (2) the multifunctional hybrid nanoprobe made the operation simpler; and (3) the PADs using urea/phenol red impregnated paper is simple and low-cost. With the resolution of detection system be further improved, this method will be widely applicable for rapid on-site detection of *S. typhimurium* and other foodborne pathogens to promote food safety and hygiene. In addition, this method provided ideas for the application of apt-Fe_3O_4@Ag NPs and PADs in the detection of other bacteria. In the future, we will further exploit the potential of apt-Fe_3O_4@Ag NPs and realize more other target detection.

Funding The authors thank the financial support from the National Natural Science Foundation of China (Grant No. 81872668), Jilin Province Development and Reform Commission (Grant No. 2019C049-3), Health commission of Jilin Province (Grant No. 2018Q033), Norman Bethune Health Science Center of Jilin University (Grant No. 2018A05), and Jilin Province Science and Technology Development Plan Item (Grant Nos. 20200602010ZP, 20200403035SF, and 20180201053SF).

Compliance with ethical standards

Conflict of interest The authors declare that they have no conflict of interest.

References

1. Ivnitski D, Abdel-Hamid I, Atanasov P, Wilkins E (1999) Biosensors for detection of pathogenic bacteria. Biosens Bioelectron 14(7):599–624
2. Zhang L, Huang R, Liu W, Liu H, Zhou X, Xing D (2016) Rapid and visual detection of listeria monocytogenes based on nanoparticle cluster catalyzed signal amplification. Biosens Bioelectron 86: 1–7
3. Jung Y et al (2019) Prevalence, levels, and viability of Salmonella in and on raw chicken livers. J Food Prot 82(5):834–843
4. Narvaez-Bravo C et al (2013) Salmonella on feces, hides and carcasses in beef slaughter facilities in Venezuela. Int J Food Microbiol 166(2):226–230
5. Salmonella. World Health Organization. Available at: http://www.topics/salmonella/en/. 2018 [cited 2020 July]
6. Kang DH, Rhee MS, Costello M (2003) Development of a miniaturized four-culture method for the rapid enumeration of four bacterial groups in ground beef. Lett Appl Microbiol 36(4):197–202
7. Singer RS, Cooke CL, Maddox CW, Isaacson RE, Wallace RL (2006) Use of pooled samples for the detection of Salmonella in feces by polymerase chain reaction. J Vet Diagn Investig 18(4): 319–325
8. Heymans R, Vila A, van Heerwaarden CAM, Jansen CCC, Castelijn GAA, van der Voort M, Biesta-Peters EG (2018) Rapid detection and differentiation of Salmonella species, Salmonella Typhimurium and Salmonella Enteritidis by multiplex quantitative PCR. PLoS One 13(10):e0206316
9. Wang S, Zheng L, Cai G, Liu N, Liao M, Li Y, Zhang X, Lin J (2019) A microfluidic biosensor for online and sensitive detection of Salmonella typhimurium using fluorescence labeling and smartphone video processing. Biosens Bioelectron 140:111333
10. Mutreja R, Jariyal M, Pathania P, Sharma A, Sahoo DK, Suri CR (2016) Novel surface antigen based impedimetric immunosensor for detection of Salmonella typhimurium in water and juice samples. Biosens Bioelectron 85:707–713
11. Bhandari D, Chen F-C, Bridgman CR (2019) Detection of Salmonella Typhimurium in romaine lettuce using a surface plasmon resonance biosensor. Biosensors 9:94
12. Morbioli GG, Mazzu-Nascimento T, Stockton AM, Carrilho E (2017) Technical aspects and challenges of colorimetric detection with microfluidic paper-based analytical devices (μPADs) - a review. Anal Chim Acta 970:1–22
13. LeVatte MA, Lipfert M, Zheng J, Wishart DS (2019) A fast, sensitive, single-step colorimetric dipstick assay for quantifying ascorbic acid in urine. Anal Biochem 580:1–13
14. Shih CM, Chang CL, Hsu MY, Lin JY, Kuan CM, Wang HK, Huang CT, Chung MC, Huang KC, Hsu CE, Wang CY, Shen YC, Cheng CM (2015) Paper-based ELISA to rapidly detect Escherichia coli. Talanta 145:2–5
15. Pang B, Zhao C, Li L, Song X, Xu K, Wang J, Liu Y, Fu K, Bao H, Song D, Meng X, Qu X, Zhang Z, Li J (2018) Development of a low-cost paper-based ELISA method for rapid Escherichia coli O157:H7 detection. Anal Biochem 542:58–62
16. Sun L, Jiang Y, Pan R, Li M, Wang R, Chen S, Fu S, Man C (2018) A novel, simple and low-cost paper-based analytical device for colorimetric detection of Cronobacter spp. Anal Chim Acta 1036: 80–88
17. Sun J, Huang J, Li Y, Lv J, Ding X (2019) A simple and rapid colorimetric bacteria detection method based on bacterial inhibition of glucose oxidase-catalyzed reaction. Talanta 197:304–309
18. Shen J, Zhu Y, Yang X, Zong J, Li C (2013) Multifunctional Fe3O4@Ag/SiO2/Au core-shell microspheres as a novel SERS-activity label via long-range plasmon coupling. Langmuir 29(2): 690–695
19. Liu J, Qiao SZ, Hu QH, Max Lu GQ (2011) Magnetic nanocomposites with mesoporous structures: synthesis and applications. Small 7(4):425–443
20. Li F, Li F, Luo D, Lai W, Xiong Y, Xu H (2018) Biotin-exposure-based immunomagnetic separation coupled with nucleic acid lateral flow biosensor for visibly detecting viable listeria monocytogenes. Anal Chim Acta 1017:48–56
21. Pang Y, Wang C, Wang J, Sun Z, Xiao R, Wang S (2016) Fe(3)O(4)@Ag magnetic nanoparticles for microRNA capture and duplex-specific nuclease signal amplification based SERS detection in cancer cells. Biosens Bioelectron 79:574–580

22. Guo Z, Xu J, Zhang J, Hu Y, Pan Y, Miao P (2018) Facile strategy for electrochemical analysis of hydrogen peroxide based on multifunctional Fe3O4@Ag nanocomposites. ACS Applied Bio Materials 1(2):367–373
23. Meng F, Zhu X, Miao P (2015) Study of autocatalytic oxidation reaction of silver nanoparticles and the application for nonenzymatic H2O2 assay. Chem Phys Lett 635:213–216
24. Mazzei L, Cianci M, Gonzalez Vara A, Ciurli S (2018) The structure of urease inactivated by Ag(i): a new paradigm for enzyme inhibition by heavy metals. Dalton Trans 47(25):8240–8247
25. Duan N et al (2016) Magnetic nanoparticles-based aptasensor using gold nanoparticles as colorimetric probes for the detection of Salmonella typhimurium. Anal Sci 32(4):431–436
26. Wu W, Li J, Pan D, Li J, Song S, Rong M, Li Z, Gao J, Lu J (2014) Gold nanoparticle-based enzyme-linked antibody-aptamer sandwich assay for detection of Salmonella Typhimurium. ACS Appl Mater Interfaces 6(19):16974–16981
27. Joshi R, Janagama H, Dwivedi HP, Senthil Kumar TMA, Jaykus LA, Schefers J, Sreevatsan S (2009) Selection, characterization, and application of DNA aptamers for the capture and detection of Salmonella enterica serovars. Mol Cell Probes 23(1):20–28
28. Zhu Y, Shen J, Zhou K, Chen C, Yang X, Li C (2011) Multifunctional magnetic composite microspheres with in situ growth au nanoparticles: a highly efficient catalyst system. J Phys Chem C 115(5):1614–1619
29. Jun B-H, Noh MS, Kim G, Kang H, Kim JH, Chung WJ, Kim MS, Kim YK, Cho MH, Jeong DH, Lee YS (2009) Protein separation and identification using magnetic beads encoded with surface-enhanced Raman spectroscopy. Anal Biochem 391(1):24–30
30. Kashefi-Kheyrabadi L, Mehrgardi MA (2012) Aptamer-conjugated silver nanoparticles for electrochemical detection of adenosine triphosphate. Biosens Bioelectron 37(1):94–98
31. Schneider CA, Rasband WS, Eliceiri KW (2012) NIH image to ImageJ: 25 years of image analysis. Nat Methods 9(7):671–675
32. Vos JJ (1978) Colorimetric and photometric properties of a 2° fundamental observer. Color Research & Application 3(3):125–128
33. Wang C, Gu B, Liu Q, Pang Y, Xiao R, Wang S (2018) Combined use of vancomycin-modified Ag-coated magnetic nanoparticles and secondary enhanced nanoparticles for rapid surface-enhanced Raman scattering detection of bacteria. Int J Nanomedicine 13:1159–1178
34. Chen D-H, Chen C-J (2002) Formation and characterization of Au–Ag bimetallic nanoparticles in water-in-oil microemulsions. J Mater Chem 12(5):1557–1562
35. Liu Y, Wang J, Zhao C, Guo X, Song X, Zhao W, Liu S, Xu K, Li J (2019) A multicolorimetric assay for rapid detection of listeria monocytogenes based on the etching of gold nanorods. Anal Chim Acta 1048:154–160
36. Kong T, You JB, Zhang B, Nguyen B, Tarlan F, Jarvi K, Sinton D (2019) Accessory-free quantitative smartphone imaging of colorimetric paper-based assays. Lab Chip 19(11):1991–1999
37. Yi J, Wu P, Li G, Xiao W, Li L, He Y, He Y, Ding P, Chen C (2019) A composite prepared from carboxymethyl chitosan and aptamer-modified gold nanoparticles for the colorimetric determination of Salmonella typhimurium. Microchim Acta 186(11):711
38. Srisa-Art M, Boehle KE, Geiss BJ, Henry CS (2018) Highly sensitive detection of Salmonella typhimurium using a colorimetric paper-based analytical device coupled with immunomagnetic separation. Anal Chem 90(1):1035–1043